CD36, but not G2A, modulates efferocytosis, inflammation, and fibrosis following bleomycin-induced lung injury[s]

Brian W. Parks,[1,]* Leland L. Black,* Kurt A. Zimmerman,[†] Allison E. Metz,[§] Chad Steele,[§] Joanne E. Murphy-Ullrich,[†] and Janusz H. Kabarowski[2,]*

Department of Microbiology,* Department of Pathology,[†] and Department of Medicine,[§] University of Alabama at Birmingham, Birmingham, AL

Abstract Macrophage G2A and CD36 lipid receptors are thought to mediate efferocytosis following tissue injury and thereby prevent excessive inflammation that could compromise tissue repair. To test this, we subjected mice lacking G2A or CD36 receptor to bleomycin-induced lung injury and measured efferocytosis, inflammation, and fibrosis. Loss of CD36 (but not G2A) delayed clearance of apoptotic alveolar cells (mean 78% increase in apoptotic cells 7 days postinjury), potentiated inflammation (mean 56% increase in lung neutrophils and 75% increase in lung KC levels 7 days postinjury, 51% increase in lung macrophages 14 days postinjury), and reduced lung fibrosis (mean 41% and 29% reduction 14 and 21 days postinjury, respectively). Reduced fibrosis in CD36$^{-/-}$ mice was associated with lower levels of profibrotic TH2 cytokines (IL-9, IL-13, IL-4), decreased expression of the M2 macrophage marker Arginase-1, and reduced interstitial myofibroblasts. G2A, on the other hand, was required for optimal clearance of apoptotic neutrophils during zymosan-induced peritoneal inflammation (50.3% increase in apoptotic neutrophils and 30.6% increase in total neutrophils 24 h following zymosan administration in G2A$^{-/-}$ mice).███ Thus, CD36 is required for timely removal of apoptotic cells in the context of lung injury and modulates subsequent inflammatory and fibrotic processes relevant to fibrotic lung disease.—Parks, B. W., L. L. Black, K. A. Zimmerman, A. E. Metz, C. Steele, J. E. Murphy-Ullrich, and J. H. Kabarowski. **CD36, but not G2A, modulates efferocytosis, inflammation, and fibrosis following bleomycin-induced lung injury.** *J. Lipid Res.* 2013. **54:** 1114–1123.

Supplementary key words lipid • receptor • apoptosis

The timely removal of apoptotic cells by phagocytic macrophages (efferocytosis) is vital for the preservation of normal tissue homeostasis (1, 2). Moreover, defects in this fundamentally important process in the context of tissue injury lead to the accumulation of necrotic cells that can exacerbate inflammation and thereby undermine normal profibrotic tissue repair (2, 3). The rapid and efficient clearance of apoptotic cells is thus vital for the normal resolution of inflammation and orchestration of subsequent tissue repair mechanisms following injury (4).

Efferocytosis involves the coordinated action of receptors mediating macrophage movement toward cells undergoing apoptosis (so-called "find-me" attraction signals) and those regulating the subsequent recognition of apoptotic cells ("eat-me" signals), leading to their engulfment (2). Phospholipid oxidation is a characteristic feature of apoptosis, resulting in the expression of lipid ligands on the surface of apoptotic cells that are recognized by macrophage CD36 scavenger receptor (5–7). Lipids liberated from cells undergoing apoptosis, on the other hand, have been proposed to mediate "find-me" attraction signals based on their potent chemotactic activity toward macrophages (8). Lysophosphatidylcholine (LPC) is one such lipid that is produced by cells undergoing apoptosis via caspase-mediated calcium-independent phospholipase-A$_2$ (iPLA$_2$) activation (9, 10) and which stimulates chemoattraction of cultured macrophages via the G2A receptor (11). As LPC is liberated from apoptotic cells in amounts sufficient to stimulate macrophage chemotaxis via G2A in vitro (10, 12), it has become widely accepted that G2A provides an important attraction signal for the recruitment of macrophages to facilitate efferocytosis (13–16). However, in vivo data supporting this notion is lacking. Similarly, an in vivo role for CD36 in efferocytosis has been demonstrated in very limited

Abbreviations: BAL, bronchoalveolar lavage; IL, interleukin; LPC, lysophosphatidylcholine; αSMA, alpha smooth muscle cell actin; TGF-β, transforming growth factor-β; TH2, T helper 2; TUNEL, terminal deoxynucleotidyl transferase-mediated dUTP nick end labeling; WT, wild-type.

[1] Current address of B. W. Parks: Department of Medicine, University of California, Los Angeles, CA.

[2] To whom correspondence should be addressed.
    e-mail: janusz@uab.edu

[s] The online version of this article (available at http://www.jlr.org) contains supplementary data in the form of one figure.

physiological and pathophysiological contexts (6), despite the fact that a large body of in vitro data point to CD36 as an important mediator of apoptotic cell recognition and uptake (3, 17, 18). Importantly, there is no in vivo evidence supporting a requirement for either CD36 or G2A receptor in efferocytosis using an animal disease model in which tissue injury and clearance of apoptotic cells was monitored in conjunction with subsequent inflammatory and fibrotic repair processes. Furthermore, previous studies of CD36-deficient (CD36$^{-/-}$) mice in certain disease models have yielded results that were unexpected based on prior in vitro data (19). In addition, functions have been ascribed to CD36 that could influence inflammation and fibrosis following tissue injury independently of its effects on efferocytosis. For example, CD36 can modify inflammation as a coreceptor for various Toll-like receptors (TLR) (20) and has also been postulated to facilitate tissue fibrosis following injury by promoting activation of the profibrotic cytokine, transforming growth factor-β (TGF-β), through direct interaction with thrombospondin-1 (TSP-1) (21, 22). However, little is known regarding the physiological relevance and functional interplay between these various properties of CD36 in vivo.

To address the need for in vivo studies to complement the significant body of in vitro data supporting a key role for CD36 and G2A receptors in efferocytosis, we used wild-type (WT), G2A-deficient (G2A$^{-/-}$) and CD36$^{-/-}$ mice to directly test whether G2A and/or CD36 receptors are required for the clearance of apoptotic cells following tissue injury in vivo and to monitor their subsequent effects on inflammation and fibrosis using the established bleomycin model of lung injury (23). The results of this study demonstrate that CD36 (but not G2A) is required for apoptotic cell clearance in the context of bleomycin-induced lung injury and that CD36 modulates subsequent inflammatory and fibrotic responses in a manner that points to this receptor as a potential therapeutic target in fibrotic pulmonary disease.

MATERIALS AND METHODS

Animals

G2A-sufficient (G2A$^{+/+}$) and G2A$^{-/-}$ mice were derived by intercrossing mice heterozygous for the G2A mutant allele (G2A$^{+/-}$) that were backcrossed greater than 10 generations onto the C57BL/6J background. CD36$^{-/-}$ mice were generously provided by Dr. Maria Febbraio (Cleveland Clinic Foundation) and were backcrossed more than six generations onto the C57BL/6J background. All mice were maintained under pathogen-free conditions, and all studies were conducted in conformity with Public Health Service (PHS) Policy on Humane Care and Use of Laboratory Animals and with approval from the Animal Care Committee of the University of Alabama at Birmingham.

Bleomycin-induced lung injury

Six- to eight-week-old male WT, G2A$^{-/-}$, and CD36$^{-/-}$ mice were challenged with a single intratracheal instillation of 5 units of bleomycin sulfate (Calbiochem) per kilogram of body weight. Bronchoalveolar lavage (BAL) samples were recovered from mice at various time points following bleomycin administration

by lung lavage with HBSS (without Ca^{2+}/Mg^{2+}). BAL fluid was centrifuged at 1,500 rpm for 5 min at 4°C, and supernatants were subsequently aliquoted and stored at −20°C. BAL cells were resuspended in FACS staining buffer (PBS/0.5% fetal calf serum) and stained with the following fluorochrome-conjugated antibodies: (stain 1) anti-CD11b^{PercP} (BD Biosciences), anti-Gr-1^{FITC} (BD Biosciences), and anti-CD115 (M-CSF receptor)^{PE} (eBioscience); and (stain 2) anti-CD4^{PerCP} (BD Biosciences), anti-CD8^{FITC} (BD Biosciences), and anti-CD19^{PE} (BD Biosciences). Total BAL cell numbers were measured using the flow cytometer, and specific cell-types were identified as follows: Neutrophils (CD11b$^+$ GR-1^{high} CD115$^-$), monocytes (CD11b$^+$ GR-1^{high} CD115$^+$), macrophages (CD11b$^+$ GR-1^{low} CD115$^+$), CD4$^+$ T cells (CD4$^+$ CD8$^-$), CD8$^+$ T cells (CD4$^-$ CD8$^+$), and B cells (CD19$^+$). Representative flow cytometric plots are shown in supplementary Fig. I. All data were analyzed using Cell Quest (BD Biosciences) and WinMDI software (Scripps Research Institute).

LPC ESI-MS/MS analysis

LPC concentration in BAL fluid was measured by ESI-MS/MS as previously described (24, 25). Briefly, total lipids were extracted, dried under nitrogen, and resuspended in methanol: chloroform (2:1 v/v). Samples were subsequently measured by direct injection using an API-4000 Q Trap Quadrupole mass spectrometer.

Cytokine analysis of BAL fluid

BAL fluid concentrations of cytokines were measured using the Bio-Plex Pro Mouse Cytokine 23-plex assay (Bio-Rad) and a Bio-Plex 200 system (Bio-Rad) according to manufacturer's instructions. TGF-β activity in 250 µl BAL fluid samples was measured as previously described using a reporter assay in mink lung epithelial cells (MLEC) stably transfected with an expression construct containing a truncated plasminogen activator inhibitor-1 (PAI-1) promoter containing a TGF-β response element fused to the firefly luciferase gene (26).

Hydroxyproline analysis of lung homogenates

Lungs were homogenized in 2 ml PBS, and 1 ml of lung homogenate was desiccated by baking at 110°C in a 4 ml glass vial. Dried lung homogenates were subsequently hydrolyzed in 1 ml 6N HCL at 110°C for 16 h. After cooling, 25 µl of hydrolyzed lung homogenate was transferred to a 5 ml glass tube, combined with 1 ml Chloramine T solution (1.4% Chloramine T, 10% 1-propanol, 0.5M sodium acetate), and incubated for 20 min at room temperature. One milliliter of Erlich's solution (1M *p*-dimethylaminobenzaldehyde, 70% 1-propanol, 20% perchloric acid) was then added and incubated for 15 min at 65°C. The solution (200 µl) was then transferred to a clear 96-well plate, and absorbance was measured at 550 nm. The amount of hydroxyproline was determined against a hydroxyproline standard curve.

Lung TUNEL, immunohistochemical, and immunofluorescence analysis

Lungs were filled with 0.8 ml of 1:1 PBS:OCT (Tissue-Tek) solution, excised from the animal, and subsequently placed in tissue blocks, covered in OCT, flash-frozen in liquid nitrogen, and stored at −80°C. For six randomly chosen male WT, G2A$^{-/-}$, and CD36$^{-/-}$ mice, 8 µm lung cryosections were stained with anti-F4/80^{Alexa555} antibody followed by terminal deoxynucleotidyl transferase-mediated dUTP nick end labeling (TUNEL) as previously described (24). Quantitation of apoptotic cells was performed by enumerating the number of TUNEL$^+$ cells per microscopic field in color images captured on an Olympus BX60 fluorescence microscope. For each mouse, eight random 100× microscopic fields

(each field containing a major airway around which TUNEL$^+$ apoptotic cells were consistently concentrated) were quantified. Trichrome staining was performed as previously described (25). For assessment of α smooth muscle cell actin (αSMA) expressing myofibroblasts in lungs of control and bleomycin-treated mice, three 8 μm lung cryosections (spaced approximately 200 μm apart) from each animal (five for each experimental group) were stained with Cy3-conjugated anti-αSMA antibody (Sigma-Aldrich; #C6198). Fluorescence intensity in images taken from three random 100× microscopic fields of each lung cryosection (each field containing a major airway) was quantified using the histogram function of Adobe Photoshop CS5.1 (Adobe Systems, San Jose, CA). The average fluorescence intensity value was measured for each field, excluding the αSMA highly expressing airway smooth muscle cells, in order to selectively quantify interstitial myofibroblasts.

Lung ARG-1 expression

10^5 BAL cells from WT, G2A$^{-/-}$, and CD36$^{-/-}$ mice (14 days following intratracheal bleomycin administration; 5 units/kg body weight) were resuspended and lysed in RIPA buffer [20 mM Tris (pH 7.4), 150 mM NaCl, 0.05% SDS, 1% Triton X-100, 10% glycerol, 0.05% protease inhibitors (Sigma #P2714)]. Equivalent amounts of total protein were subsequently separated by SDS-PAGE and immunoblotted with antibody against ARG-1 (BD Biosciences #610708). Immunoreactive bands were visualized using enhanced chemiluminescence and quantified densitometrically using ImageJ software (National Institutes of Health).

Zymosan-induced peritonitis

Mice were injected intraperitoneally with 1 mg of Zymosan A (Sigma-Aldrich) in PBS. At indicated time points (0, 6, 24, and 48 h), mice were euthanized and peritonea were flushed with 5 ml HBSS. Peritoneal exudate cells were counted using a hemocytometer, stained with anti-Gr-1^{FITC} and anti-CD115^{APC} antibodies, washed, and subsequently stained with Annexin-V^{PE} and 7-AAD according to the manufacturers protocol (BD Biosciences). Cells were analyzed using a FACS Calibur flow cytometer. Neutrophils and macrophages were identified as Gr-1$^+$ CD115$^-$ and Gr-1$^+$ CD115$^+$, respectively. Apoptotic and necrotic cells were identified as Annexin-V$^+$ 7-AAD$^-$ and Annexin-V$^+$ 7-AAD$^+$, respectively. Data were acquired from a total of 10^5 peritoneal cells from each zymosan-injected animal. For each genotype (WT, G2A$^{-/-}$, and CD36$^{-/-}$), nine or more animals were analyzed at each time point (0, 6, 24, and 48 h).

Statistical analysis

Statistical analysis was performed using SigmaStat (Systat Software, Inc.). Student *t*-test was used for single comparisons and one-way ANOVA (ANOVA) was used for multiple comparisons. For all statistical analyses, $P < 0.05$ was considered significant.

RESULTS

Loss of CD36, but not G2A, delays apoptotic cell clearance following bleomycin-induced lung injury

We addressed the requirement for G2A and CD36 receptors using a physiologically relevant in vivo model of lung injury in which apoptosis of resident cells was induced and the kinetics of their subsequent clearance measured over time. Intratracheal bleomycin instillation is a widely employed model for the study of pulmonary inflammation and fibrosis associated with injury, in which initial alveolar

epithelial and endothelial cell apoptosis is associated with inflammatory cell recruitment, followed by apoptotic cell clearance, resolution of inflammation, and the orchestration of tissue repair mechanisms characterized by excessive fibrosis (23). We measured the kinetics of apoptotic alveolar cell clearance following bleomycin-induced lung injury in WT, G2A$^{-/-}$, and CD36$^{-/-}$ mice. Prior to bleomycin instillation (5 units/kg body weight), the lungs of WT, G2A$^{-/-}$, and CD36$^{-/-}$ mice contained comparable numbers of terminal deoxynucleotidyl transferase-mediated dUTP nick end labeling-positive (TUNEL$^+$) apoptotic cells (**Fig. 1A**). An approximately 13-fold increase in TUNEL$^+$ apoptotic cells was observed in the lungs of WT, G2A$^{-/-}$, and CD36$^{-/-}$ mice two days following bleomycin instillation, and no significant effect of G2A deficiency or CD36 deficiency on the extent of bleomycin-induced apoptosis was detected at this time point (Fig. 1A). However, CD36 deficiency significantly delayed the subsequent clearance of these apoptotic cells (mean 78% increase in apoptotic cells seven days postinjury in CD36$^{-/-}$ mice) (Fig. 1A, B).
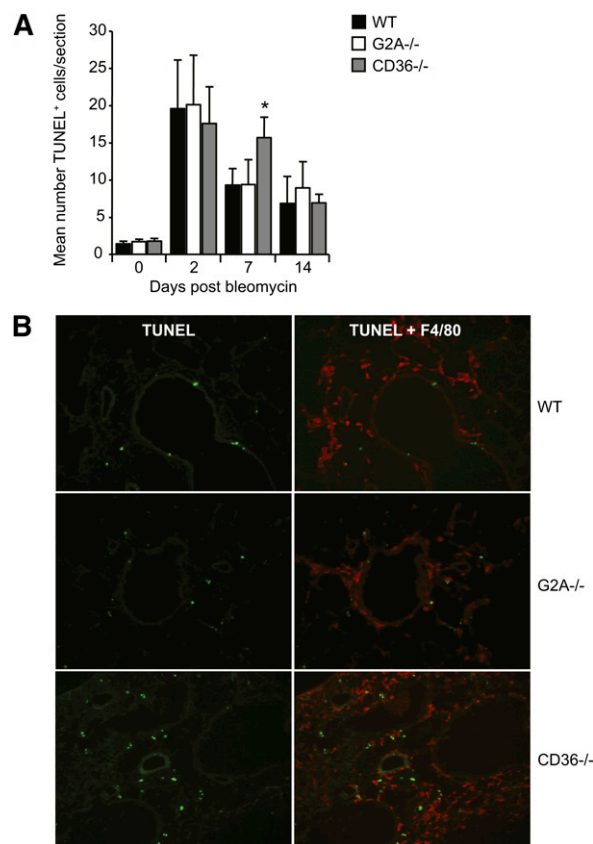

Fig. 1. Delayed clearance of apoptotic alveolar cells in lungs of bleomycin-treated CD36$^{-/-}$, but not G2A$^{-/-}$, mice. (A) Average number of TUNEL$^+$ apoptotic cells in sections of lung from WT, G2A$^{-/-}$, and CD36$^{-/-}$ mice prepared at the indicated time points following intratracheal bleomycin (5 units/kg body weight) administration. Data shown are average ± SD of six mice for each genotype at each time point (*$P < 0.05$). (B) Representative immunofluorescence images of TUNEL$^+$ (green) apoptotic cells and F4/80$^+$ macrophages in lung sections from WT, G2A$^{-/-}$, and CD36$^{-/-}$ mice seven days following intratracheal bleomycin administration (100× magnification).

G2A deficiency, on the other hand, had no such effect (Fig. 1A, B), despite robust increases in bronchoalveolar lavage (BAL) fluid LPC concentrations beginning two days following bleomycin instillation (coincident with the induction of apoptosis) (**Fig. 2**).

Increased bronchoalveolar neutrophil and macrophage numbers following bleomycin-induced lung injury in CD36$^{-/-}$ mice

The chemotactic function of G2A has been postulated to contribute to the recruitment of monocytes and T cells into sites of inflammation in response to locally generated LPC (11, 16, 27). G2A deficiency may thus modulate the induction and/or resolution of inflammation following bleomycin-induced lung injury. Furthermore, defective apoptotic cell clearance in CD36$^{-/-}$ mice (Fig. 1A, B) could result in the amplification and/or protraction of inflammation (28, 29). To address these issues, we measured bronchoalveolar inflammatory cell composition in WT, G2A$^{-/-}$, and CD36$^{-/-}$ mice by flow cytometry at various time points following bleomycin instillation (staining regimen for identification of neutrophils, monocytes, and macrophages shown in supplementary Fig. I). Comparable increases in bronchoalveolar neutrophils, monocytes, CD4$^+$ T cells, CD8$^+$ T cells, and B cells were detected in WT, G2A$^{-/-}$, and CD36$^{-/-}$ mice 2 days following bleomycin instillation (**Fig. 3**). G2A deficiency had no significant impact on neutrophil, monocyte, CD4$^+$ T cell, CD8$^+$ T cell, or B cell numbers at later time points and did not affect bronchoalveolar macrophage numbers (Fig. 3). Taken together, these data demonstrate that G2A signaling is redundant for normal apoptotic cell clearance following bleomycin-induced lung injury and does not modify the initiation or resolution of inflammation in this model. CD36 deficiency, however, resulted in significant increases

in neutrophils and macrophages 7 days and 14 days following bleomycin instillation, respectively (Fig. 3).

Multiplex analysis of BAL cytokine levels revealed elevated levels of the neutrophilic chemokine KC (CXCL1) in CD36$^{-/-}$ mice (mean 75% and 42% increases 7 and 14 days postinjury, respectively; 29% increase at day 2 not significant) (**Fig. 4A**). In addition, levels of interleukin (IL)-13, IL-4, IL-9, and IL-5 (profibrotic TH2-type cytokines) (30) were present at lower levels in CD36$^{-/-}$ mice compared with their WT counterparts at certain time points following bleomycin instillation (Fig. 4B). BAL levels of active transforming growth factor-β (TGF-β), a major profibrotic cytokine (31), were also reduced in CD36$^{-/-}$ mice 7 days (but not 14 days) following bleomycin treatment (Fig. 4C). The remaining cytokines measured in the multiplex assay (IL-1α, IL-1β, IL-2, IL-3, IL-6, IL-10, IL-12p40, IL-12p70, IL-17, Eotaxin, RANTES, G-CSF, GM-CSF, Interferon-γ, MCP-1, MIP-1α, MIP-1β, and TNFα) were unaffected by CD36 deficiency at any time point examined (data not shown). Thus, in CD36$^{-/-}$ mice, delayed apoptotic cell clearance was associated with significant increases in bronchoalveolar neutrophils, coincident with elevated levels of KC (CXCL1), higher bronchoalveolar macrophage numbers and reduced profibrotic TH2 cytokines. In G2A$^{-/-}$ mice, on the other hand, no significant differences in the levels of any cytokine other than IL-5 were detected between WT and G2A$^{-/-}$ mice (Fig. 4), consistent with the absence of any effect of G2A deficiency on apoptotic cell clearance or cellular features of inflammation following bleomycin-induced lung injury (Figs. 1 and 3).

Reduced lung fibrosis in bleomycin-treated CD36$^{-/-}$ mice

The significantly greater bronchoalveolar neutrophil and macrophage numbers in bleomycin-treated CD36$^{-/-}$
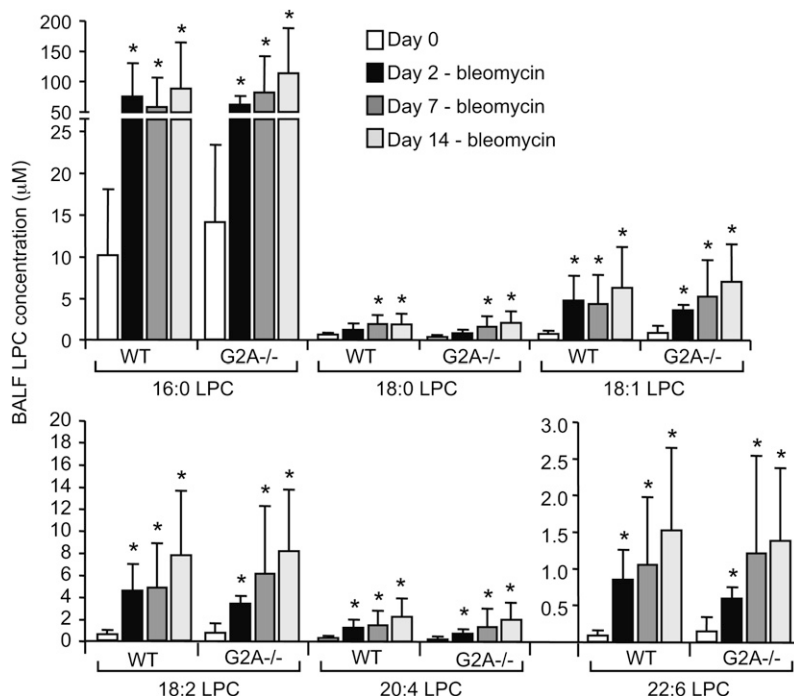

Fig. 2. Major LPC species are increased in bronchoalveolar fluid (BALF) following intratracheal bleomycin administration in WT and G2A$^{-/-}$ mice. Data are average ± SD of 5 animals for each time point (*$P < 0.05$ relative to day 0 control).
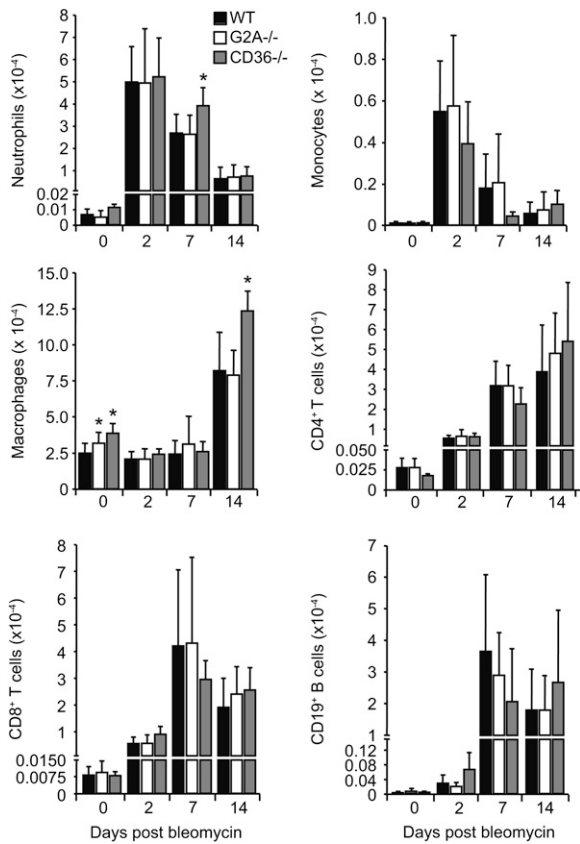
Fig. 3. Increased inflammation in lungs of bleomycin-treated CD36$^{-/-}$ mice. Absolute numbers of the indicated cell types in BAL fluid from WT, G2A$^{-/-}$, and CD36$^{-/-}$ mice at the indicated time points following intratracheal bleomycin (5 units/kg body weight) administration. Note increased neutrophil and macrophage numbers in CD36$^{-/-}$ mice at 7 and 14 days postbleomycin treatment. Data are average ± SD of six animals for each genotype at each time point (*$P < 0.05$).

Fig. 4. Levels of the indicated cytokines in BAL fluid from WT, G2A$^{-/-}$, and CD36$^{-/-}$ mice at the indicated time points following intratracheal bleomycin (5 units/kg body weight) administration. (A) Significantly increased levels of the proinflammatory neutrophilic chemokine KC (CXCL1) in CD36$^{-/-}$ mice. (*$P < 0.05$ relative to WT). (B) Levels of TH2-type cytokines in BAL fluid from WT, G2A$^{-/-}$, and CD36$^{-/-}$ mice at the indicated time points following intratracheal bleomycin (5 units/kg body weight) administration. Significantly reduced levels of IL-9, IL-13, IL-4, and IL-5 at various time points following bleomycin treatment. (*$P < 0.05$, §$P = 0.053$). (C) TGF-β activity in BAL fluid from WT, G2A$^{-/-}$, and CD36$^{-/-}$ mice at the indicated time points following intratracheal bleomycin (5 units/kg body weight) administration. Data are average ± SD of five animals for each genotype at each time point.

mice (Fig. 3), indicative of increased inflammation, and their reduced levels of profibrotic TH2 cytokines, which are known to promote alternative profibrotic M2 macrophage activation (30) (Fig. 4B, C), suggested that lung fibrosis may be reduced in these animals. Indeed, defective apoptotic cell clearance can prevent the polarization of macrophages to a profibrotic M2 phenotype, thus impairing the orchestration of fibrotic repair processes (32). Furthermore, a direct profibrotic role for CD36 following bleomycin-induced lung injury has been proposed through its interaction with thrombospondin-1 (TSP-1) and resulting induction of active TGF-β (21, 22). We therefore measured the hydroxyproline content of lungs, a quantitative measure of fibrosis (23), from WT, G2A$^{-/-}$, and CD36$^{-/-}$ mice 14 and 21 days following bleomycin instillation. While lung hydroxyproline content was unaffected by G2A deficiency, CD36$^{-/-}$ mice had significant reductions in hydroxyproline, indicative of reduced fibrosis (**Fig. 5A**). Consistent with this observation, trichrome-stained sections of lung from the same CD36$^{-/-}$ mice exhibited less extensive areas of collagen deposition (Fig. 5B). Finally, consistent with reduced M2 macrophage polarization, expression of the M2 macrophage marker, Arginase-1 (ARG-1), was significantly
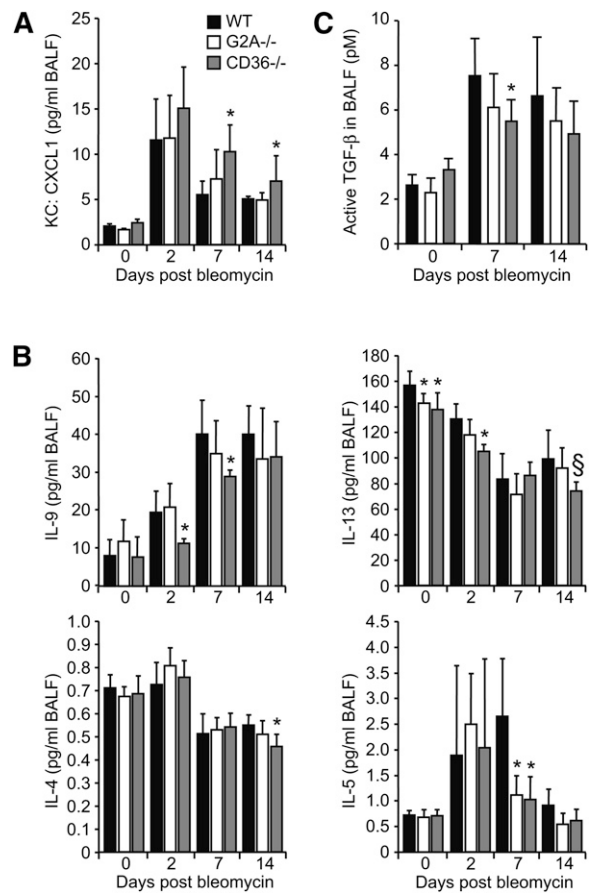
reduced in bronchoalveolar cells from CD36$^{-/-}$ mice 14 days following bleomycin-induced lung injury (Fig. 5C).

The reduced levels of TH2 cytokines and active TGF-β observed in bleomycin treated CD36$^{-/-}$ mice may collectively contribute to the less fibrotic milieu in these animals. As αSMA-positive myofibroblasts are major cellular mediators of fibrosis following bleomycin-induced injury (33, 34) and because their differentiation is regulated to a significant extent by TH2 cytokines (35, 36), we assessed lung interstitial αSMA expression to determine whether the reduced fibrosis in CD36$^{-/-}$ mice was associated with decreased numbers of myofibroblasts. Significant reductions in αSMA expressing interstitial myofibroblasts (independent of airway smooth muscle staining) were observed in the lungs of CD36$^{-/-}$ mice compared with their WT counterparts 14 days following intratracheal bleomycin administration (**Fig. 6**).
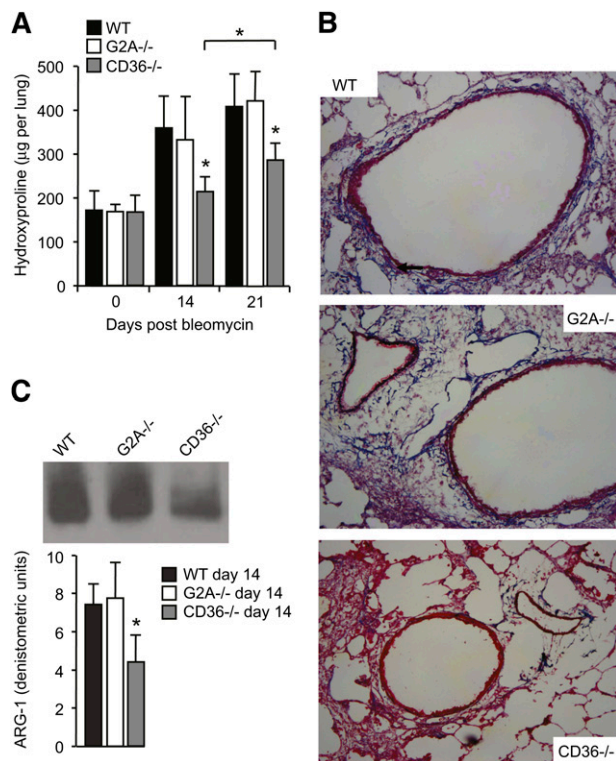
Fig. 5. Reduced lung fibrosis in bleomycin-treated CD36$^{-/-}$ mice. (A) Hydroxyproline content of lungs from control and bleomycin-treated (5 units/kg body weight) WT, G2A$^{-/-}$, and CD36$^{-/-}$ mice (average ± SD of five animals for each genotype at each time point, *P < 0.05). (B) Representative trichrome-stained sections form lungs of WT, G2A$^{-/-}$, and CD36$^{-/-}$ mice 14 days following intratracheal bleomycin administration (200× magnification). Blue (collagen). (C) ARG-1 protein expression in BAL cells from the indicated mice 14 days following bleomycin treatment (5 units/kg body weight). Representative Western blots showing ARG-1 protein levels shown above. Data shown is the average ± SD of three animals for each genotype (*P < 0.05).

Delayed clearance of neutrophils in zymosan-treated G2A$^{-/-}$ mice

Frasch et al. reported that antibody-mediated G2A blockade or genetic deletion of G2A both significantly delay the clearance of neutrophils in the murine zymosan-induced peritoneal inflammation model (37, 38). In the latter, more recent study, both viable and apoptotic neutrophils were identified and enumerated by morphological examination in peritoneal exudate cytospin preparations from wild-type and G2A$^{-/-}$ animals; both viable and apoptotic neutrophil populations were found to be significantly increased 18–48 h following intraperitoneal zymosan injection (38). Thus, we considered why G2A deficiency did not affect bronchoalveolar neutrophil numbers following bleomycin instillation in our present study (Fig. 3). Furthermore, we reasoned that in addition to elevated production of the neutrophilic chemokine KC (CXCL1) (Fig. 4A), defective neutrophil clearance may have contributed to the increased neutrophil numbers observed following bleomycin-induced lung injury in CD36$^{-/-}$ mice (Fig. 3). To address these issues, we measured the kinetics of neutrophil clearance following intraperitoneal zymosan injection in

WT, G2A$^{-/-}$, and CD36$^{-/-}$ mice (n ⩾ 9 for each genotype). To accurately identify and quantify apoptotic versus viable neutrophils in peritoneal exudates, we employed a flow cytometric approach similar to that employed for the examination of BAL cells in supplementary Fig. I in combination with Annexin-V staining. Robust neutrophilic inflammation was elicited within 6 h of intraperitoneal zymosan injection, which was almost completely resolved by 48 h in WT, G2A$^{-/-}$, and CD36$^{-/-}$ mice (**Fig. 7A**). In G2A$^{-/-}$ mice, however, the kinetics of neutrophil clearance was significantly attenuated (mean 30.6% increase in peritoneal neutrophils 24 h following zymosan injection) (Fig. 7A), and this was associated with increases of both apoptotic (Annexin-V$^+$ 7AAD$^-$, mean 50.3% increase) and postapoptotic/necrotic (Annexin-V$^+$ 7AAD$^+$, mean 42.9% increase) neutrophils (Fig. 7B). In CD36$^{-/-}$ mice, on the other hand, we did not detect any impairment of neutrophil clearance (Fig. 7). Interestingly, numbers of postapoptotic/necrotic (but not apoptotic) neutrophils were significantly reduced in CD36$^{-/-}$ mice 6 h (but not at any other time point) following intraperitoneal zymosan injection (mean 55% decrease) (Fig. 7B), suggesting either a reduced rate of postapoptotic neutrophil necrosis or an increased clearance of postapoptotic/necrotic neutrophils in the absence of CD36.

DISCUSSION

A role for CD36 in apoptotic cell clearance in vivo has hitherto only been demonstrated in a skin punch wound healing assay using CD36$^{-/-}$ mice (6). The fact that CD36 was required for optimal apoptotic cell clearance following bleomycin-induced lung injury (Fig. 1) is therefore an important finding, particularly as other receptors in addition to CD36 are likely involved and may have been predicted to obscure any effects of CD36 deficiency (i.e., make CD36 functionally redundant in this model) (2). Indeed, similar effects on efferocytosis and lung inflammation were recently reported for the MER tyrosine kinase receptor in mice following bleomycin-induced lung injury (39). The modulatory effects of CD36 on subsequent inflammatory and fibrotic events also reveal the importance of this receptor in regulating processes that are pathophysiologically relevant to idiopathic pulmonary fibrosis (IPF). Notably, the reduced rate of apoptotic cell clearance in the lungs of bleomycin-treated CD36$^{-/-}$ mice was associated with an increase in neutrophils (on day 7 postintratracheal bleomycin administration) and macrophages (on day 14) that could not be explained by increased initial neutrophil and monocyte infiltration (on day 2) (Fig. 3). However, multiplex analysis of BAL fluid cytokine levels did reveal significantly higher levels of the neutrophilic chemokine KC (CXCL1) in bleomycin-treated CD36$^{-/-}$ mice 7 and 14 days postbleomycin treatment (Fig. 4A). KC (CXCL1) is a potent chemokine for neutrophils whose receptor was shown to be important for neutrophilic recruitment into the airways of bleomycin-treated mice (40). While the main source of this increased bronchoalveolar CXCL1 in CD36$^{-/-}$ mice remains to be determined, it is possible that
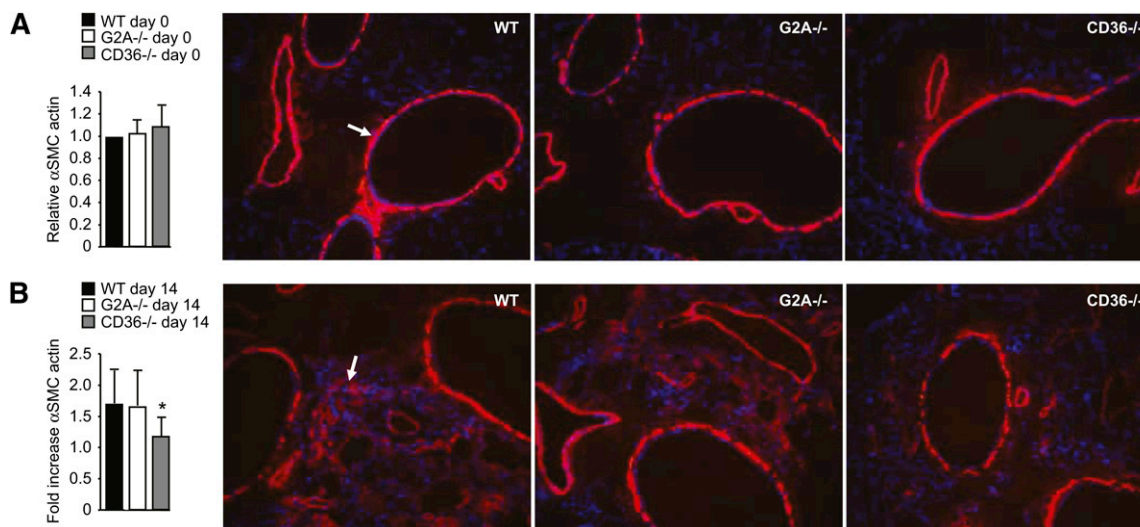
Fig. 6. Reduced αSMA expressing myofibroblasts in lungs of bleomycin-treated CD36$^{-/-}$ mice. (A) Relative fluorescence intensity of αSMA staining in control (day 0) WT, G2A$^{-/-}$, and CD36$^{-/-}$ mice. Representative αSMA-stained sections shown alongside (100× magnification). Arrow indicates airway smooth muscle cell staining that was excluded in the quantification of interstitial αSMA staining. (B) Fold increase in fluorescence intensity of αSMA staining in bleomycin-treated (5 units/kg body weight; day 14) WT, G2A$^{-/-}$, and CD36$^{-/-}$ mice compared with their genotypically matched controls (day 0). Representative αSMA-stained sections shown alongside (100× magnification). Red, αSMA; blue, Hoechst-stained nuclei. Arrow indicates αSMA expressing interstitial myofibroblasts. Data shown are average ± SD of five animals for each genotype at each time point (*$P < 0.05$).

an increase in CXCL1-mediated neutrophil recruitment, rather than a decrease in neutrophil clearance, may contribute to the augmented neutrophilic inflammation observed in CD36$^{-/-}$ mice following lung injury. Indeed, this is supported by our failure to detect a suppressive effect of CD36 deficiency on neutrophil clearance in the zymosan-induced peritoneal inflammation model (Fig. 7). However, we cannot exclude the possibility that impaired clearance of neutrophils resulting from loss of CD36-mediated interaction with NADPH oxidase-generated oxidized phospholipids (37) could have contributed to increasing neutrophils in the lungs of bleomycin-treated CD36$^{-/-}$ mice, despite the lack of a similar effect in the zymosan-induced peritoneal inflammation model.

It was somewhat surprising that, despite the widely held notion that G2A is involved in the clearance of apoptotic cells (2, 13, 14), we found that G2A deficiency had no significant effect on apoptotic cell clearance in the bleomycin-induced lung injury model (Fig. 1). Indeed, although an LPC-dependent chemotactic function of G2A has been described in monocytes/macrophages and T cells in vitro (11, 16, 27), we did not detect any significant effect of G2A deficiency on the frequency of bronchoalveolar monocytes, macrophages, T cells, or neutrophils following bleomycin-induced lung injury (Fig. 3), despite demonstrable increases in local LPC production (Fig. 2). In this regard, it may be noteworthy that published studies of G2A deficiency in mouse models of inflammatory diseases associated with local generation of LPC, such as atherosclerosis and multiple sclerosis, have similarly failed to provide evidence that either the efferocytic or chemotactic roles for G2A are important in vivo (41–43). Moreover, considering that defective apoptotic cell clearance has been linked to breakage of immune tolerance and the development of

autoimmunity (44, 45), it is interesting that no evidence for an increased predisposition of G2A$^{-/-}$ mice to autoimmunity compared with their age, gender, and genetically matched WT counterparts has been reported (46). Nevertheless, in this present study, we were able to provide important confirmatory data supporting a key role for G2A in apoptotic neutrophil clearance in the zymosan-induced peritoneal inflammation model (Fig. 7) as originally reported by Frasch et al. (37, 38). This, in conjunction with data from the bleomycin-induced lung injury model, further underscores the potential degree of context-dependent functional redundancy between these receptors in terms of their requirement for efferocytosis in vivo. Indeed, while it is widely accepted that the in vivo relevance of individual receptors is likely to be determined to a significant extent by the context, tissue, and cell-type in which apoptosis occurs, published comparative studies similar to ours employing in vivo models that directly address this issue are lacking.

Impaired apoptotic cell clearance in CD36$^{-/-}$ mice was associated with augmented lung inflammation following bleomycin-induced injury (Fig. 3) and subsequently a reduced fibrotic response (Fig. 5A). Several studies have reported a similar association between increased lung inflammation and reduced fibrosis following lung injury (47). Moreover, increased macrophage infiltration and reduced fibrosis was reported in the kidneys of CD36$^{-/-}$ mice following unilateral ureteral obstruction (48). One could therefore speculate that an abnormal accumulation of apoptotic cells in the lungs of bleomycin-treated CD36$^{-/-}$ mice may have prevented the timely resolution of inflammation, leading to the impairment of subsequent fibrotic changes (4, 35). Furthermore, defective apoptotic cell clearance can promote the polarization of macrophages to a
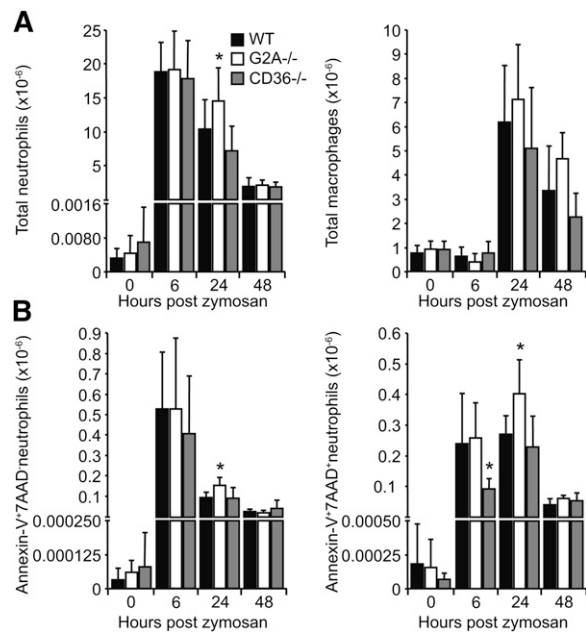
Fig. 7. Impaired neutrophil clearance in G2A$^{-/-}$, but not CD36$^{-/-}$, mice following zymosan-induced peritoneal inflammation. (A) Absolute numbers of peritoneal neutrophils and macrophages at the indicated time points following intraperitoneal zymosan injection (1 mg). (B) Absolute numbers of peritoneal apoptotic neutrophils (Annexin-V$^+$ 7AAD$^-$ Gr-1$^+$ CD115$^-$) and postapoptotic/necrotic neutrophils (Annexin-V$^+$ 7AAD$^+$ Gr-1$^+$ CD115$^-$) at the indicated time points following intraperitoneal zymosan injection. Note significant delay in neutrophil clearance in G2A$^{-/-}$ mice in (A) and increased numbers of apoptotic neutrophils in the same mice in (B). Data are average ± SD of at least 8 animals for each genotype at each time point (15, 12, and 11 WT, G2A$^{-/-}$, and CD36$^{-/-}$ mice, respectively, at 24 h postzymosan injection) (*$P <$ 0.05).

proinflammatory M1 phenotype, thus delaying transition to a fibrotic repair stage normally promoted by M2 macrophage polarization (32). Indeed, we found significantly reduced expression of the M2 marker ARG-1 in BAL cells from CD36$^{-/-}$ mice compared with their WT and G2A$^{-/-}$ counterparts (Fig. 5C). However, the reduced fibrosis in CD36$^{-/-}$ mice may equally reflect other recognized functions of CD36 independent of its role in efferocytosis. Indeed, it is unclear to what extent defective apoptotic cell clearance in CD36$^{-/-}$ mice contributed to the proinflammatory and antifibrotic changes. Delineating the interrelationships between these processes will be difficult considering that the response to lung injury is complex, involving the coordinated action of multiple cytokines/chemokines, inflammatory cells, and resident epithelial, endothelial, and fibroblastic cells (23). The effects of CD36 on lung inflammation and fibrosis may thus be multifactorial, involving multiple cell types as well as multiple functional properties of CD36 (some possibly operational in the same cell type) (20, 49). For example, CD36 has been identified as a coreceptor for various Toll-like receptors (TLR) in macrophages promoting inflammation in response to endogenous CD36 ligands (20). CD36 deficiency could therefore influence inflammatory processes independently of its impairment of apoptotic cell clearance following bleomycin-induced

lung injury. Indeed, the neutrophilic chemokine, CXCL1, was significantly increased in the lungs of bleomycin-treated CD36$^{-/-}$ mice compared with their WT and G2A$^{-/-}$ counterparts (Fig. 4A), and it is known that KC (CXCL1) production by resident tissue macrophages is controlled by signaling from TLRs (50). In addition, studies with peptides blocking CD36 interaction with TSP-1 suggest that CD36/TSP-1 signaling is important for the activation of TGF-β following bleomycin-induced lung injury (21, 22). Consistent with this, decreased lung fibrosis in CD36$^{-/-}$ mice following bleomycin treatment was associated with a reduction in bronchoalveolar levels of active TGF-β at day 7 (Fig. 4C). Although the moderate extent to which active TGF-β was reduced in CD36$^{-/-}$ mice may be somewhat surprising considering the aforementioned peptide blocking studies (21, 22), it is noteworthy that genetic deletion of TSP-1 did not reduce active TGF-β or attenuate lung fibrosis following bleomycin-induced lung injury either (51). Similarly to TSP-1 (51), therefore, our data show that global CD36 deficiency, as opposed to selective disruption of CD36/TSP1 interaction, does not have a robust suppressive effect on levels of active TGF-β following bleomycin-induced lung injury (Fig. 4C). This in turn suggests that the reduced lung fibrosis in CD36$^{-/-}$ mice may occur through the combined cumulative effects of reduced TH2 cytokines (IL-9, IL-13, IL-4, IL-5) and TGF-β (Fig. 4B, C). Indeed, polarization to a TH2-type response or inactivation of TH2-type cytokines (IL-4, IL-13, or IL-9) can promote or inhibit, respectively, pulmonary fibrosis in mice following bleomycin-induced lung injury (52–55). The profibrotic effects of these TH2 cytokines are mediated in part by their ability to promote the differentiation and proliferation of collagen-producing myofibroblasts (35). Thus, our finding that αSMA-expressing myofibroblasts were significantly reduced in the lungs of bleomycin-treated CD36$^{-/-}$ mice compared with their WT counterparts (Fig. 6) may be mechanistically relevant. Further studies are required to dissect the molecular and cellular pathways by which CD36 signaling regulates this cell type. In addition, other lipid-mediated mechanisms may account for the association between reduced efferocytosis and reduced fibrosis in CD36$^{-/-}$ mice, including increased local generation of PGE2 by macrophages in response to increased numbers of apoptotic cells (56, 57). Indeed, PGE2 produced as a result of the abnormal accumulation of apoptotic cells may act directly on myofibroblasts themselves to mediate antifibrotic effects (58, 59).

Finally, whether G2A and/or CD36 receptors are required or functionally redundant for efferocytosis may depend to a significant degree on the types of lipids generated by the apoptotic cell as well as those associated with the local inflammatory milieu. In addition to quantitative and qualitative differences in lipid composition of the apoptotic cell, the nature of the inflammatory milieu (cytokine expression, involvement of TLR signaling, macrophage M1 versus M2 phenotype) may also be a major determinant of receptor function in efferocytosis. Characterization of lipid species generated in different models in vivo in conjunction with an accurate assessment of macrophage

phenotype may therefore provide important mechanistic insights into this fundamental issue. Furthermore, as underscored by our findings, a complete understanding of the relevance and functional redundancy between major receptors mediating "find-me" and "eat-me" signals will necessitate the utilization of multiple in vivo models of tissue injury and inflammation in addition to macrophage-specific genetic manipulation in order to separate their roles in efferocytosis from effects in other tissues. The cumulative data from such studies will also lead to a much better understanding of the extent to which deregulation of individual pathways contributes to the pathology of chronic inflammatory diseases in which defective apoptotic cell clearance has been implicated as an etiological factor. In this regard, our findings identify the CD36 receptor as a potential target for therapeutic intervention in fibrotic lung diseases, such as chronic obstructive pulmonary disease (COPD), and warrant further studies to delineate the key cellular and molecular mechanisms responsible among a potential pleiotropy of CD36 functions (20, 49).

REFERENCES

1. Henson, P. M., and D. A. Hume. 2006. Apoptotic cell removal in development and tissue homeostasis. *Trends Immunol.* **27:** 244–250.
2. Ravichandran, K. S., and U. Lorenz. 2007. Engulfment of apoptotic cells: signals for a good meal. *Nat. Rev. Immunol.* **7:** 964–974.
3. Fadok, V. A., M. L. Warner, D. L. Bratton, and P. M. Henson. 1998. CD36 is required for phagocytosis of apoptotic cells by human macrophages that use either a phosphatidylserine receptor or the vitronectin receptor (alpha v beta 3). *J. Immunol.* **161:** 6250–6257.
4. Henson, P. M., R. W. Vandivier, and I. S. Douglas. 2006. Cell death, remodeling, and repair in chronic obstructive pulmonary disease? *Proc. Am. Thorac. Soc.* **3:** 713–717.
5. Podrez, E. A., E. Poliakov, Z. Shen, R. Zhang, Y. Deng, M. Sun, P. J. Finton, L. Shan, B. Gugiu, P. L. Fox, et al. 2002. Identification of a novel family of oxidized phospholipids that serve as ligands for the macrophage scavenger receptor CD36. *J. Biol. Chem.* **277:** 38503–38516.
6. Greenberg, M. E., M. Sun, R. Zhang, M. Febbraio, R. Silverstein, and S. L. Hazen. 2006. Oxidized phosphatidylserine-CD36 interactions play an essential role in macrophage-dependent phagocytosis of apoptotic cells. *J. Exp. Med.* **203:** 2613–2625.
7. Hazen, S. L. 2008. Oxidized phospholipids as endogenous pattern recognition ligands in innate immunity. *J. Biol. Chem.* **283:** 15527–15531.
8. Muñoz, L. E., C. Peter, M. Herrmann, S. Wesselborg, and K. Lauber. 2010. Scent of dying cells: the role of attraction signals in the clearance of apoptotic cells and its immunological consequences. *Autoimmun. Rev.* **9:** 425–430.
9. Kim, S. J., D. Gershov, X. Ma, N. Brot, and K. B. Elkon. 2002. I-PLA(2) activation during apoptosis promotes the exposure of membrane lysophosphatidylcholine leading to binding by natural immunoglobulin M antibodies and complement activation. *J. Exp. Med.* **196:** 655–665.
10. Lauber, K., E. Bohn, S. M. Krober, Y. J. Xiao, S. G. Blumenthal, R. K. Lindemann, P. Marini, C. Wiedig, A. Zobywalski, S. Baksh, et al. 2003. Apoptotic cells induce migration of phagocytes via caspase-3-mediated release of a lipid attraction signal. *Cell.* **113:** 717–730.
11. Yang, L. V., C. G. Radu, L. Wang, M. Riedinger, and O. N. Witte. 2005. Gi-independent macrophage chemotaxis to lysophosphatidylcholine via the immunoregulatory GPCR G2A. *Blood.* **105:** 1127–1134.
12. Peter, C., M. Waibel, C. G. Radu, L. V. Yang, O. N. Witte, K. Schulze-Osthoff, S. Wesselborg, and K. Lauber. 2008. Migration to apoptotic "find-me" signals is mediated via the phagocyte receptor G2A. *J. Biol. Chem.* **283:** 5296–5305.
13. Peter, C., S. Wesselborg, M. Herrmann, and K. Lauber. 2010. Dangerous attraction: phagocyte recruitment and danger signals of apoptotic and necrotic cells. *Apoptosis.* **15:** 1007–1028.
14. Elliott, M. R., and K. S. Ravichandran. 2010. Clearance of apoptotic cells: implications in health and disease. *J. Cell Biol.* **189:** 1059–1070.
15. Nagata, S., R. Hanayama, and K. Kawane. 2010. Autoimmunity and the clearance of dead cells. *Cell.* **140:** 619–630.
16. Kabarowski, J. H. 2009. G2A and LPC: regulatory functions in immunity. *Prostaglandins Other Lipid Mediat.* **89:** 73–81.
17. Fadok, V. A., D. L. Bratton, D. M. Rose, A. Pearson, R. A. Ezekewitz, and P. M. Henson. 2000. A receptor for phosphatidylserine-specific clearance of apoptotic cells. *Nature.* **405:** 85–90.
18. Moodley, Y., P. Rigby, C. Bundell, S. Bunt, H. Hayashi, N. Misso, R. McAnulty, G. Laurent, A. Scaffidi, P. Thompson, et al. 2003. Macrophage recognition and phagocytosis of apoptotic fibroblasts is critically dependent on fibroblast-derived thrombospondin 1 and CD36. *Am. J. Pathol.* **162:** 771–779.
19. Witztum, J. L. 2005. You are right too! *J. Clin. Invest.* **115:** 2072–2075.
20. Stewart, C. R., L. M. Stuart, K. Wilkinson, J. M. van Gils, J. Deng, A. Halle, K. J. Rayner, L. Boyer, R. Zhong, W. A. Frazier, et al. 2010. CD36 ligands promote sterile inflammation through assembly of a Toll-like receptor 4 and 6 heterodimer. *Nat. Immunol.* **11:** 155–161.
21. Yehualaeshet, T., R. O'Connor, A. Begleiter, J. E. Murphy-Ullrich, R. Silverstein, and N. Khalil. 2000. A CD36 synthetic peptide inhibits bleomycin-induced pulmonary inflammation and connective tissue synthesis in the rat. *Am. J. Respir. Cell Mol. Biol.* **23:** 204–212.
22. Chen, Y., X. Wang, D. Weng, L. Tian, L. Lv, S. Tao, and J. Chen. 2009. A TSP-1 synthetic peptide inhibits bleomycin-induced lung fibrosis in mice. *Exp. Toxicol. Pathol.* **61:** 59–65.
23. Moore, B. B., and C. M. Hogaboam. 2008. Murine models of pulmonary fibrosis. *Am. J. Physiol. Lung Cell. Mol. Physiol.* **294:** L152–L160.
24. Parks, B. W., G. P. Gambill, A. J. Lusis, and J. H. Kabarowski. 2005. Loss of G2A promotes macrophage accumulation in atherosclerotic lesions of low density lipoprotein receptor-deficient mice. *J. Lipid Res.* **46:** 1405–1415.
25. Parks, B. W., A. J. Lusis, and J. H. Kabarowski. 2006. Loss of the lysophosphatidylcholine effector, G2A, ameliorates aortic atherosclerosis in low-density lipoprotein receptor knockout mice. *Arterioscler. Thromb. Vasc. Biol.* **26:** 2703–2709.
26. Abe, M., J. G. Harpel, C. N. Metz, I. Nunes, D. J. Loskutoff, and D. B. Rifkin. 1994. An assay for transforming growth factor-beta using cells transfected with a plasminogen activator inhibitor-1 promoter-luciferase construct. *Anal. Biochem.* **216:** 276–284.
27. Radu, C. G., L. V. Yang, M. Riedinger, M. Au, and O. N. Witte. 2004. T cell chemotaxis to lysophosphatidylcholine through the G2A receptor. *Proc. Natl. Acad. Sci. USA.* **101:** 245–250.
28. Mukaro, V. R., and S. Hodge. 2011. Airway clearance of apoptotic cells in COPD. *Curr. Drug Targets.* **12:** 460–468.
29. Krysko, O., P. Vandenabeele, D. V. Krysko, and C. Bachert. 2010. Impairment of phagocytosis of apoptotic cells and its role in chronic airway diseases. *Apoptosis.* **15:** 1137–1146.
30. Gordon, S. 2003. Alternative activation of macrophages. *Nat. Rev. Immunol.* **3:** 23–35.
31. Border, W. A., and N. A. Noble. 1994. Transforming growth factor beta in tissue fibrosis. *N. Engl. J. Med.* **331:** 1286–1292.
32. Mares, C. A., J. Sharma, Q. Li, E. L. Rangel, E. G. Morris, M. I. Enriquez, and J. M. Teale. 2011. Defect in efferocytosis leads to alternative activation of macrophages in Francisella infections. *Immunol. Cell Biol.* **89:** 167–172.
33. Li, Y., D. Jiang, J. Liang, E. B. Meltzer, A. Gray, R. Miura, L. Wogensen, Y. Yamaguchi, and P. W. Noble. 2011. Severe lung fibrosis requires an invasive fibroblast phenotype regulated by hyaluronan and CD44. *J. Exp. Med.* **208:** 1459–1471.
34. Zhang, K., M. D. Rekhter, D. Gordon, and S. H. Phan. 1994. Myofibroblasts and their role in lung collagen gene expression during pulmonary fibrosis. A combined immunohistochemical and in situ hybridization study. *Am. J. Pathol.* **145:** 114–125.
35. Wilson, M. S., and T. A. Wynn. 2009. Pulmonary fibrosis: pathogenesis, etiology and regulation. *Mucosal Immunol.* **2:** 103–121.
36. Ingram, J. L., A. B. Rice, K. Geisenhoffer, D. K. Madtes, and J. C. Bonner. 2004. IL-13 and IL-1beta promote lung fibroblast growth

through coordinated up-regulation of PDGF-AA and PDGF-Ralpha. *FASEB J.* **18:** 1132–1134.

37. Frasch, S. C., K. Z. Berry, R. Fernandez-Boyanapalli, H. S. Jin, C. Leslie, P. M. Henson, R. C. Murphy, and D. L. Bratton. 2008. NADPH oxidase-dependent generation of lysophosphatidylserine enhances clearance of activated and dying neutrophils via G2A. *J. Biol. Chem.* **283:** 33736–33749.

38. Frasch, S. C., R. F. Fernandez-Boyanapalli, K. Z. Berry, C. C. Leslie, J. V. Bonventre, R. C. Murphy, P. M. Henson, and D. L. Bratton. 2011. Signaling via macrophage G2A enhances efferocytosis of dying neutrophils by augmentation of Rac activity. *J. Biol. Chem.* **286:** 12108–12122.

39. Lee, Y. J., S. H. Lee, Y. S. Youn, J. Y. Choi, K. S. Song, M. S. Cho, and J. L. Kang. 2012. Preventing cleavage of Mer promotes efferocytosis and suppresses acute lung injury in bleomycin treated mice. *Toxicol. Appl. Pharmacol.* **263:** 61–72.

40. Russo, R. C., R. Guabiraba, C. C. Garcia, L. S. Barcelos, E. Roffe, A. L. Souza, F. A. Amaral, D. Cisalpino, G. D. Cassali, A. Doni, et al. 2009. Role of the chemokine receptor CXCR2 in bleomycin-induced pulmonary inflammation and fibrosis. *Am. J. Respir. Cell Mol. Biol.* **40:** 410–421.

41. Parks, B. W., R. Srivastava, S. Yu, and J. H. Kabarowski. 2009. ApoE-dependent modulation of HDL and atherosclerosis by G2A in LDL receptor-deficient mice independent of bone marrow-derived cells. *Arterioscler. Thromb. Vasc. Biol.* **29:** 539–547.

42. Osmers, I., S. S. Smith, B. W. Parks, S. Yu, R. Srivastava, J. E. Wohler, S. R. Barnum, and J. H. Kabarowski. 2009. Deletion of the G2A receptor fails to attenuate experimental autoimmune encephalomyelitis. *J. Neuroimmunol.* **207:** 18–23.

43. Bolick, D. T., M. D. Skaflen, L. E. Johnson, S. C. Kwon, D. Howatt, A. Daugherty, K. S. Ravichandran, and C. C. Hedrick. 2009. G2A deficiency in mice promotes macrophage activation and atherosclerosis. *Circ. Res.* **104:** 318–327.

44. Steinman, R. M., S. Turley, I. Mellman, and K. Inaba. 2000. The induction of tolerance by dendritic cells that have captured apoptotic cells. *J. Exp. Med.* **191:** 411–416.

45. Savill, J., I. Dransfield, C. Gregory, and C. Haslett. 2002. A blast from the past: clearance of apoptotic cells regulates immune responses. *Nat. Rev. Immunol.* **2:** 965–975.

46. Srivastava, R., S. Yu, B. W. Parks, L. L. Black, and J. H. Kabarowski. 2011. Autoimmune-mediated reduction of high-density lipoprotein-cholesterol and paraoxonase 1 activity in systemic lupus erythematosus-prone gld mice. *Arthritis Rheum.* **63:** 201–211.

47. Shvedova, A. A., E. R. Kisin, A. R. Murray, C. Kommineni, V. Castranova, B. Fadeel, and V. E. Kagan. 2008. Increased accumulation of neutrophils and decreased fibrosis in the lung of NADPH oxidase-deficient C57BL/6 mice exposed to carbon nanotubes. *Toxicol. Appl. Pharmacol.* **231:** 235–240.

48. Okamura, D. M., S. Pennathur, K. Pasichnyk, J. M. Lopez-Guisa, S. Collins, M. Febbraio, J. Heinecke, and A. A. Eddy. 2009. CD36 regulates oxidative stress and inflammation in hypercholesterolemic CKD. *J. Am. Soc. Nephrol.* **20:** 495–505.

49. Miller, Y. I., S. H. Choi, P. Wiesner, L. Fang, R. Harkewicz, K. Hartvigsen, A. Boullier, A. Gonen, C. J. Diehl, X. Que, et al. 2011. Oxidation-specific epitopes are danger-associated molecular patterns recognized by pattern recognition receptors of innate immunity. *Circ. Res.* **108:** 235–248.

50. De Filippo, K., R. B. Henderson, M. Laschinger, and N. Hogg. 2008. Neutrophil chemokines KC and macrophage-inflammatory protein-2 are newly synthesized by tissue macrophages using distinct TLR signaling pathways. *J. Immunol.* **180:** 4308–4315.

51. Ezzie, M. E., M. G. Piper, C. Montague, C. A. Newland, J. M. Opalek, C. Baran, N. Ali, D. Brigstock, J. Lawler, and C. B. Marsh. 2011. Thrombospondin-1 deficient mice are not protected from bleomycin-induced pulmonary fibrosis. *Am. J. Respir. Cell Mol. Biol.* **44:** 556–561.

52. Xu, J., A. L. Mora, J. LaVoy, K. L. Brigham, and M. Rojas. 2006. Increased bleomycin-induced lung injury in mice deficient in the transcription factor T-bet. *Am. J. Physiol. Lung Cell. Mol. Physiol.* **291:** L658–L667.

53. Huaux, F., T. Liu, B. McGarry, M. Ullenbruch, and S. H. Phan. 2003. Dual roles of IL-4 in lung injury and fibrosis. *J. Immunol.* **170:** 2083–2092.

54. Belperio, J. A., M. Dy, M. D. Burdick, Y. Y. Xue, K. Li, J. A. Elias, and M. P. Keane. 2002. Interaction of IL-13 and C10 in the pathogenesis of bleomycin-induced pulmonary fibrosis. *Am. J. Respir. Cell Mol. Biol.* **27:** 419–427.

55. Arras, M., J. Louahed, J. F. Heilier, M. Delos, F. Brombacher, J. C. Renauld, D. Lison, and F. Huaux. 2005. IL-9 protects against bleomycin-induced lung injury: involvement of prostaglandins. *Am. J. Pathol.* **166:** 107–115.

56. Charbeneau, R. P., and M. Peters-Golden. 2005. Eicosanoids: mediators and therapeutic targets in fibrotic lung disease. *Clin. Sci. (Lond.).* **108:** 479–491.

57. Medeiros, A. I., C. H. Serezani, S. P. Lee, and M. Peters-Golden. 2009. Efferocytosis impairs pulmonary macrophage and lung antibacterial function via PGE2/EP2 signaling. *J. Exp. Med.* **206:** 61–68.

58. Huang, S. K., S. H. Wettlaufer, J. Chung, and M. Peters-Golden. 2008. Prostaglandin E2 inhibits specific lung fibroblast functions via selective actions of PKA and Epac-1. *Am. J. Respir. Cell Mol. Biol.* **39:** 482–489.

59. Huang, S. K., E. S. White, S. H. Wettlaufer, H. Grifka, C. M. Hogaboam, V. J. Thannickal, J. C. Horowitz, and M. Peters-Golden. 2009. Prostaglandin E(2) induces fibroblast apoptosis by modulating multiple survival pathways. *FASEB J.* **23:** 4317–4326.